SHAPE RECONSTRUCTIONS OF SOUND - SOFT OBSTACLES BURIED IN ARBITRARILY SHAPED PENETRABLE CYLINDERS

F. Yaman Istanbul Technical University Electrical-Electronics Eng. Faculty, Istanbul, TURKEY
A. Yapar Istanbul Technical University Electrical-Electronics Eng. Faculty, Istanbul, TURKEY

1 INTRODUCTION

In this study an integral equation based method is presented to reconstruct the location and shape of sound-soft obstacles buried in penetrable cylinders from limited or full far field data. The direct scattering problem considered for this configuration is to obtain the scattered far field in the case of acoustic time harmonic plane wave incidence. The inverse problem is the reconstruction of two dimensional shape of the buried scatterer from the far field data. For a solution of the direct and the inverse problems a Potential (Layer) approach is used to obtain system of boundary integral equations. Numerical solutions of the integral equations which contains a singular kernel is achieved by Nyström method and Tikhonov regularization is used for the solution of the first kind integral equations. Numerical simulations are carried out to test the feasibility and the applicability of the method.

2 GENERAL FORMULATION

Let $\boldsymbol{D}_0$ denotes a doubly connected, bounded medium $\boldsymbol{D}_0 \subset \mathrm{IR}^2$, with a smooth boundary $\partial \boldsymbol{D}_0$, which consists of an interior boundary Γ_0 and an exterior boundary Γ_1 such that $\partial \boldsymbol{D} = \Gamma_0 \cup \Gamma_1$ and $\Gamma_0 \cap \Gamma_1 = \varnothing$. We shall denote the unit normal of the boundary Γ_0 directed into interior of $\boldsymbol{D}_0$ by ν_0 and the unit normal of the boundary Γ_1 directed into exterior of $\boldsymbol{D}_0$ by ν_1. λ is a complex valued continuous function defined on Γ_1 which has a sufficiently small norm for the penetration of the exterior field to the domain $\boldsymbol{D}_0$. The interior total field $\boldsymbol{u}_0 \in \boldsymbol{C}^2(\boldsymbol{D}_0) \cap \boldsymbol{C}^1\left(\overline{\boldsymbol{D}_0}\right)$ and the exterior total field $\boldsymbol{u}_1 \in \boldsymbol{C}^2(\boldsymbol{D}_1) \cap \boldsymbol{C}^1\left(\overline{\boldsymbol{D}_1}\right)$ have to satisfy the Helmholtz equations

$$\Delta \boldsymbol{u}_m + \boldsymbol{k}_m^2 \boldsymbol{u}_m = 0 \qquad \text{in } \boldsymbol{D}_m \qquad \boldsymbol{m} = 0,\ 1 \tag{1}$$

where $\boldsymbol{k}_m$ is the wave number of the corresponding medium defined as $\boldsymbol{k}_m = \omega / \boldsymbol{c}_m$. Here $\omega > 0$ is the frequency and $\boldsymbol{c}_m$ is the speed of the sound in the related medium.
We consider the conductive boundary condition satisfied on the boundary Γ_1 and the Dirichlet boundary condition on the Γ_0 that lead to the equations

$$\boldsymbol{u}_1 = \boldsymbol{u}_0 \qquad \text{and} \qquad \frac{\partial \boldsymbol{u}_1}{\partial \nu_1} - \frac{\partial \boldsymbol{u}_0}{\partial \nu_1} = \lambda \boldsymbol{u}_1 \quad \text{on} \quad \Gamma_1, \tag{2}$$

$$\boldsymbol{u}_0 = 0 \quad \text{on} \quad \Gamma_0 \ . \tag{3}$$

The exterior total field $\boldsymbol{u}_1$, is decomposed as $\boldsymbol{u}_1 = \boldsymbol{u}^i + \boldsymbol{u}^s$. Here, $\boldsymbol{u}^i$ denotes time harmonic plane wave, such that $\boldsymbol{u}^i = \boldsymbol{e}^{i k_1 \boldsymbol{x}.\boldsymbol{d}}$, where $\boldsymbol{d} = (\cos\phi_0, \sin\phi_0)$ is the propagation direction with the angle ϕ_0, and $\boldsymbol{u}^s$ is the scattered field that satisfies the Sommerfeld radiation condition at infinity,

$$\lim_{x\to\infty}\sqrt{r}\left(\frac{\partial u^s}{\partial r}-ik_1u^s\right)=0,\qquad r=|x|\ . \tag{4}$$

Additionally it is known that every radiating solution of the scattered field has an asymptotic behavior of an outgoing wave

$$u^s(x)=\frac{e^{ik_1|x|}}{\sqrt{|x|}}\left\{u_\infty(\hat{x})+O\left(\frac{1}{|x|}\right)\right\},\qquad |x|\to\infty, \tag{5}$$

uniformly in all directions $\hat{x}=x/|x|$, where the function u_∞ defined on the unit circle Ω and is called the far field pattern of u^s.

For the solution of the direct and inverse problems the potential approach will be applied. Along this line, let Γ_j and Γ_ℓ be closed bounded curves and f be a given integrable function. The single- and double- layer integral operators can be defined as[3,4],

$$\left(S_{j\ell,m}f\right)(x):=2\int_{\Gamma_j}\Phi_m(x,y)f(y)ds(y)\ ,\qquad x\in\Gamma_\ell \tag{6}$$

$$\left(K_{j\ell,m}f\right)(x):=2\int_{\Gamma_j}\frac{\partial\Phi_m(x,y)}{\partial\nu_j(y)}f(y)ds(y)\ ,\qquad x\in\Gamma_\ell \tag{7}$$

and the corresponding normal derivative operators

$$\left(K'_{j\ell,m}f\right)(x):=2\int_{\Gamma_j}\frac{\partial\Phi_m(x,y)}{\partial\nu_\ell(x)}f(y)ds(y)\ ,\qquad x\in\Gamma_\ell \tag{8}$$

$$\left(T_{j\ell,m}f\right)(x):=2\frac{\partial}{\partial\nu_\ell(x)}\int_{\Gamma_j}\frac{\partial\Phi_m(x,y)}{\partial\nu_j(y)}f(y)ds(y)\ ,\qquad x\in\Gamma_\ell \tag{9}$$

where the sub-indices $(j,\ell)\in\{0,1\}$. Here, $\Phi_m(x,y)$ is the fundamental solution to the two-dimensional Helmholtz equation, in the domain D_m for $m=0,1$ in terms of Hankel function $H_0^{(1)}$ of the first kind and zero order, defined as

$$\Phi_m(x,y):=\frac{i}{4}H_0^{(1)}\left(k_m|x-y|\right)\qquad x\neq y\ . \tag{10}$$

The behavior of the surface potentials at the boundary is described by regularity and jump relations see[1].

We assume that the boundary curves are parametrized in the form

$$\Gamma_j=\left\{z_j(t):t\in[0,2\pi]\right\}\qquad j=0,1 \tag{11}$$

where z_j are 2π - periodic and twice continuously differentiable functions satisfying $z_j\neq 0$. For the parametrization of the integral operators see[3,4].

3 THE DIRECT PROBLEM

The scattered field $\boldsymbol{u}^{\boldsymbol{s}}$, and the interior total field $\boldsymbol{u}_0$ can be expressed in the form of combined double- and single- layer potentials

$$\boldsymbol{u}^{\boldsymbol{s}}(\boldsymbol{x}) = \int_{\Gamma_1} \left\{ \frac{\partial \Phi_1(\boldsymbol{x},\boldsymbol{y})}{\partial \nu_1(\boldsymbol{y})} \psi(\boldsymbol{y}) + \Phi_1(\boldsymbol{x},\boldsymbol{y}) \varphi(\boldsymbol{y}) \right\} \boldsymbol{ds}(\boldsymbol{y}) \ , \quad \boldsymbol{x} \in \boldsymbol{D}_1 \ , \tag{12}$$

$$\boldsymbol{u}_0(\boldsymbol{x}) = \int_{\Gamma_1} \left\{ \frac{\partial \Phi_0(\boldsymbol{x},\boldsymbol{y})}{\partial \nu_1(\boldsymbol{y})} \psi(\boldsymbol{y}) + \Phi_0(\boldsymbol{x},\boldsymbol{y}) \varphi(\boldsymbol{y}) \right\} \boldsymbol{ds}(\boldsymbol{y}) + \int_{\Gamma_0} \Phi_0(\boldsymbol{x},\boldsymbol{y}) \chi(\boldsymbol{y}) \boldsymbol{ds}(\boldsymbol{y}) \ , \quad \boldsymbol{x} \in \boldsymbol{D}_0 \,. \tag{13}$$

We note that this representation of the fields solve the direct scattering problem uniquely provided that the continuous densities ψ, φ, and χ satisfy the following integral equation system,

$$\left(\boldsymbol{K}_{11,1} - \boldsymbol{K}_{11,0} + 2\boldsymbol{I}\right)\psi + \left(\boldsymbol{S}_{11,1} - \boldsymbol{S}_{11,0}\right)\varphi - \boldsymbol{S}_{01,0}\chi = -2\boldsymbol{u}^{\boldsymbol{i}}\big|_{\Gamma_1} , \tag{14}$$

$$\left(\boldsymbol{T}_{11,1} - \boldsymbol{T}_{11,0} - \lambda \boldsymbol{K}_{11,1} - \lambda\right)\psi + \left(\boldsymbol{K}'_{11,1} - \boldsymbol{K}'_{11,0} - \lambda \boldsymbol{S}_{11,1} - 2\boldsymbol{I}\right)\varphi + \boldsymbol{K}'_{01,0}\chi = 2\left(\lambda \boldsymbol{u}^{\boldsymbol{i}}\big|_{\Gamma_1} - \frac{\partial \boldsymbol{u}^{\boldsymbol{i}}}{\partial \boldsymbol{v}_1}\bigg|_{\Gamma_1} \right) , \tag{15}$$

$$\boldsymbol{K}_{10,0}\psi + \boldsymbol{S}_{10,0}\varphi + \boldsymbol{S}_{00,0}\chi = 0 \ . \tag{16}$$

The equation system is derived by applying the conductive boundary condition (2) and the Dirichlet boundary condition (3) to the integral representation of the fields $\boldsymbol{u}^{\boldsymbol{s}}$ and $\boldsymbol{u}_0$ via jump relations. To write the system in an abbreviated form we introduce the operators $\boldsymbol{E}$ and $\boldsymbol{A}$ by

$$\boldsymbol{E} := \begin{pmatrix} 2\boldsymbol{I} & 0 & 0 \\ \lambda \boldsymbol{I} & 2\boldsymbol{I} & 0 \\ 0 & 0 & 0 \end{pmatrix}, \quad \boldsymbol{A} := \begin{pmatrix} \boldsymbol{K}_{11,1} - \boldsymbol{K}_{11,0} & \boldsymbol{S}_{11,1} - \boldsymbol{S}_{11,0} & -\boldsymbol{S}_{01,0} \\ -\boldsymbol{T}_{11,1} + \boldsymbol{T}_{11,0} + \lambda \boldsymbol{K}_{11,1} & -\boldsymbol{K}'_{11,1} + \boldsymbol{K}'_{11,0} + \lambda \boldsymbol{S}_{11,1} & -\boldsymbol{K}'_{01,0} \\ \boldsymbol{K}_{10,0} & \boldsymbol{S}_{10,0} & \boldsymbol{S}_{00,0} \end{pmatrix} . \tag{17}$$

where $\boldsymbol{I}$ is the identitiy operator. Now, the system (14-16) can be written in a compact from as,

$$\left(\boldsymbol{E} + \boldsymbol{A}\right) \begin{pmatrix} \psi \\ \varphi \\ \chi \end{pmatrix} = -2 \begin{pmatrix} \boldsymbol{u}^{\boldsymbol{i}}\big|_{\Gamma_1} \\ \lambda \boldsymbol{u}^{\boldsymbol{i}}\big|_{\Gamma_1} - \dfrac{\partial \boldsymbol{u}^{\boldsymbol{i}}}{\partial \boldsymbol{v}_1}\bigg|_{\Gamma_1} \\ 0 \end{pmatrix} . \tag{18}$$

To be able to get an exponential convergence in the direct problem we make use of the Nyström Method[1] for numerical solution. Once the densities ψ and φ are obtained from the equation (18), the far field can be computed from the following representation by using trapezoidal rule,

$$\boldsymbol{u}_\infty(\hat{\boldsymbol{x}}) = \frac{\boldsymbol{e}^{-\boldsymbol{i}\pi/4}}{\sqrt{8\pi \boldsymbol{k}_1}} \int_{\Gamma_1} \left\{ \boldsymbol{k}_1 \hat{\boldsymbol{x}} \cdot \nu_1(\boldsymbol{y}) \psi(\boldsymbol{y}) + \boldsymbol{i}\varphi(\boldsymbol{y}) \right\} \boldsymbol{e}^{\boldsymbol{i}\boldsymbol{k}_1 \hat{\boldsymbol{x}}\cdot\boldsymbol{y}} \boldsymbol{ds}(\boldsymbol{y}) \ , \quad \boldsymbol{x} \in \Omega \ . \tag{19}$$

We used following tests for the accuracy of our forward code. We reduce our direct problem to a transmission problem by omitting the sound-soft obstacle in the geometry of the problem and setting $\lambda = 0$ in the equation (2). Then, we compared our results with the Method of Moments (MoM) and observed that the results obtained by two different methods are comparable. Moreover as a second test we reduced the problem given in the reference[3] by setting the impedance function zero and observe that both results matched accurately.

4 THE INVERSE PROBLEM

The inverse problem considered here is to find the shape and the location of an obstacle buried in a given bounded penetrable medium from the far field pattern for one incident wave. To this aim, we consider an arbitrarily shaped smooth boundary $\Gamma^{(0)}$ in the interior of the penetrable medium as an initial guess with a regular parameterization such that

$$\Gamma^{(0)} = \left\{ \boldsymbol{z}^{(0)}(\boldsymbol{t}) : \boldsymbol{t} \in [0, 2\pi] \right\} , \tag{20}$$

where $\boldsymbol{z}^{(0)}$ is a 2π - periodic function defined in $\mathrm{IR} \to \mathrm{IR}^2$. The reconstruction algorithm is based on the minimization of the geometrical difference between the exact shape, and the updated shape $\Gamma^{(j)}$, in the $\boldsymbol{j}^{th}$ iteration via linearized Newton method [2,4].

In order to avoid inverse crime we represent the scattered field and the interior total field by using only single layer potentials as

$$\boldsymbol{u}^s(\boldsymbol{x}) = \int_{\Gamma_1} \Phi_1(\boldsymbol{x},\boldsymbol{y}) \varphi(\boldsymbol{y}) \boldsymbol{ds}(\boldsymbol{y}) , \qquad \boldsymbol{x} \in \boldsymbol{D}_1 , \tag{21}$$

$$\boldsymbol{u}_0^{(j)}(\boldsymbol{x}) = \int_{\Gamma_1} \Phi_0(\boldsymbol{x},\boldsymbol{y}) \psi^{(j)}(\boldsymbol{y}) \boldsymbol{ds}(\boldsymbol{y}) + \int_{\Gamma^{(j)}} \Phi_0(\boldsymbol{x},\boldsymbol{y}) \chi^{(j)}(\boldsymbol{y}) \boldsymbol{ds}^{(j)}(\boldsymbol{y}) \quad , \quad \boldsymbol{x} \in \boldsymbol{D}_0 . \tag{22}$$

From the asymptotic behavior of the single layer potential, the far field operator is introduced by

$$(\boldsymbol{S}_\infty \varphi)(\hat{\boldsymbol{x}}) := \frac{\boldsymbol{e}^{i\pi/4}}{\sqrt{8\pi \boldsymbol{k}_1}} \int_{\Gamma_1} \boldsymbol{e}^{-i\boldsymbol{k}_1 \hat{\boldsymbol{x}} \cdot \boldsymbol{y}} \varphi(\boldsymbol{y}) \boldsymbol{ds}(\boldsymbol{y}) , \qquad \hat{\boldsymbol{x}} \in \Omega , \tag{23}$$

which leads to following integral equation of the first kind

$$\boldsymbol{u}_\infty = \boldsymbol{S}_\infty \varphi . \tag{24}$$

The far field equation has an analytic kernel, therefore it is severely ill-posed. Hence, Tikhonov regularization is applied to get a stable solution of the density φ. That is the ill-posed equation is replaced by

$$\alpha_1 \varphi + \boldsymbol{S}_\infty^* \boldsymbol{S}_\infty \varphi = \boldsymbol{S}_\infty^* \boldsymbol{u}_\infty \tag{25}$$

with a parameter $\alpha_1 > 0$ and the adjoint operator $\boldsymbol{S}_\infty^*$. The fields given by (21) and (22) solve the inverse scattering problem (1-3) provided that the densities satisfy the following system

$$\begin{pmatrix} \boldsymbol{S}_{11,0} & \boldsymbol{S}_{j1,0} \\ (\boldsymbol{K}'_{11,0} + \boldsymbol{I}) & \boldsymbol{K}'_{j1,0} \end{pmatrix} \begin{pmatrix} \psi^{(j)} \\ \chi^{(j)} \end{pmatrix} = \begin{pmatrix} 2\boldsymbol{u}^i\big|_{\Gamma_1} + \boldsymbol{S}_{11,1}\varphi \\ 2\dfrac{\partial \boldsymbol{u}^i}{\partial \nu_1}\bigg|_{\Gamma_1} - 2\lambda \boldsymbol{u}^i\big|_{\Gamma_1} + (\boldsymbol{K}'_{11,1} - \boldsymbol{S}_{11,1} - \boldsymbol{I})\varphi \end{pmatrix} , \tag{26}$$

which is obtained by using the conductive boundary conditions (2) and the jump relations. We applied second Tikhonov regularization to the equation (26) because of the ill-posed character of the density $\chi^{(j)}$. By using values of the densities $\psi^{(j)}$ and $\chi^{(j)}$ the interior total field and its normal derivative on the boundary $\Gamma^{(j)}$ can be computed through jump relations,

$$\boldsymbol{u}_o^{(j)}(\boldsymbol{x}) = \int_{\Gamma_1} \Phi_0(\boldsymbol{x},\boldsymbol{y}) \psi^{(j)}(\boldsymbol{y}) \boldsymbol{ds}(\boldsymbol{y}) + \int_{\Gamma^{(j)}} \Phi_0(\boldsymbol{x},\boldsymbol{y}) \chi^{(j)}(\boldsymbol{y}) \boldsymbol{ds}^{(j)}(\boldsymbol{y}) \qquad \text{on} \quad \Gamma^{(j)} , \tag{27}$$

and

$$\frac{\partial \boldsymbol{u}_0^{(j)}}{\partial \nu^{(j)}}(\boldsymbol{x}) = \int_{\Gamma_1} \frac{\partial \Phi_0(\boldsymbol{x},\boldsymbol{y})}{\partial \nu_1(\boldsymbol{x})} \psi^{(j)}(\boldsymbol{y}) \boldsymbol{ds}(\boldsymbol{y}) + \int_{\Gamma^{(j)}} \frac{\partial \Phi_0(\boldsymbol{x},\boldsymbol{y})}{\partial \nu^{(j)}(\boldsymbol{x})} \chi^{(j)}(\boldsymbol{y}) \boldsymbol{ds}^{(j)}(\boldsymbol{y}) - \frac{1}{2}\chi^{(j)}(\boldsymbol{y}) \quad \text{on} \quad \Gamma^{(j)} . \quad (28)$$

Now a parameter $\boldsymbol{h}^{(j)}$ can be computed from the following equation

$$\boldsymbol{u}_0^{(j)} \circ \boldsymbol{z}^{(j)} + \frac{\partial \boldsymbol{u}_0^{(j)}}{\partial \nu^{(j)}} \circ \boldsymbol{z}^{(j)} \boldsymbol{h}^{(j)} = 0 , \quad \text{on} \quad \Gamma^{(j)} , \quad \boldsymbol{j} = 0,1,\ldots,\boldsymbol{J}, \quad (29)$$

to update the initial guessed curve in the form

$$\Gamma^{(j+1)} = \left\{ \boldsymbol{z}^{(j+1)}(\boldsymbol{t}) = \boldsymbol{z}^{(j)}(\boldsymbol{t}) + \boldsymbol{h}^{(j)}(\boldsymbol{t}) \nu^{(j)}(\boldsymbol{t}) : \boldsymbol{t} \in [0,2\pi] \right\} , \quad (30)$$

where $\nu^{(j)}$ denotes the outward normal vector to $\Gamma^{(j)}$ and $\boldsymbol{h} : \mathrm{IR} \to \mathrm{IR}$ is sufficiently small 2π periodic function. This equation can be considered as a Taylor expansion of the $\boldsymbol{u}_0^{(j)}$ over the boundary $\Gamma^{(j)}$. The reconstruction of the update function with the equation (29) will be sensitive to errors in normal derivative of the approximate total field $\boldsymbol{u}_0^{(j)}$ in the vicinity of zeros. To obtain more stable solutions we express the unknown update function in terms of trigonometric polynomials,

$$\boldsymbol{h}^{(j)}(\boldsymbol{t}) = \sum_{\boldsymbol{r}=-\boldsymbol{R}}^{\boldsymbol{R}} \boldsymbol{a}_{\boldsymbol{r}}^{(j)} \cos \boldsymbol{r}\,\boldsymbol{t} + \boldsymbol{b}_{\boldsymbol{r}}^{(j)} \sin \boldsymbol{r}\,\boldsymbol{t} \quad , \quad \boldsymbol{t} \in [0,2\pi] . \quad (31)$$

Then we satisfy the equation (29) in the least squares sense, that is, we determine the coefficients $\left(\boldsymbol{a}_{\boldsymbol{r}}^{(j)}, \boldsymbol{b}_{\boldsymbol{r}}^{(j)}\right)$ in (31) such that for $\boldsymbol{N}$ collocation points $\boldsymbol{t}_1, \boldsymbol{t}_2, \ldots \boldsymbol{t}_{\boldsymbol{n}}, \ldots, \boldsymbol{t}_{\boldsymbol{N}}$ the least squares sum

$$\sum_{\boldsymbol{n}=1}^{\boldsymbol{N}} \left| \boldsymbol{u}_0^{(j)}\left(\boldsymbol{z}^{(j)}(\boldsymbol{t}_{\boldsymbol{n}})\right) + \frac{\partial \boldsymbol{u}_0^{(j)}}{\partial \nu}\left(\boldsymbol{z}^{(j)}(\boldsymbol{t}_{\boldsymbol{n}})\right) \sum_{\boldsymbol{r}=-\boldsymbol{R}}^{\boldsymbol{R}} \left(\boldsymbol{a}_{\boldsymbol{r}}^{(j)} \cos \boldsymbol{r}\,\boldsymbol{t}_{\boldsymbol{n}} + \boldsymbol{b}_{\boldsymbol{r}}^{(j)} \sin \boldsymbol{r}\,\boldsymbol{t}_{\boldsymbol{n}}\right) \right|^2 \quad (32)$$

is minimized. Here $\boldsymbol{t}_{\boldsymbol{n}} = 2\boldsymbol{n}\pi/\boldsymbol{N}$ and $\boldsymbol{n} = 0,1,2,\ldots,\boldsymbol{N}$. The number of basis functions $\boldsymbol{R}$ in (32) can also be considered as a kind of regularization parameter. The next iteration will start by solving the equation (26) with the updated boundary and the iterations will continue until the reconstructed curve converges to a reasonable shape, $\Gamma^{(\boldsymbol{J})} \approx \Gamma_0$.

The above reconstruction method can be summarized as follows:

1. Choose an initial guessed boundary $\Gamma^{(0)}$ with a regular parameterization as given in (20),
2. Find the density φ by solving the integral equation (25),
3. Solve the equation system (26) for the densities $\psi^{(j)}$ and $\chi^{(j)}$ in the sense of Tikhonov,
4. Using computed densities in Step(3) calculate the interior total field (27) and its normal derivative (28),
5. Find the update function $\boldsymbol{h}^{(j)}$ in (29) by minimizing the functional (32),
6. Update the boundary $\Gamma^{(j)}$ (30) and repeat Steps 3 to 6 until desired accuracy obtained.

5 NUMERICAL RESULTS

In this section we will test the proposed reconstruction method. In all applications integral equation systems are solved through the Nyström method with a discretization number $\boldsymbol{N} = 128$, and for the inverse problems circles are used as initially guessed boundaries with $\boldsymbol{J} = 10$ iterations. Regularization parameters for the equations (25) and (26) are denoted as α_1 and α_2, respectively. In order to obtain noisy far field data, random errors are added pointwise to $\boldsymbol{u}_\infty$ to have a noise level of 3% [3,4]. In the following figures line styles are chosen as dots to indicate the reconstructions with noisy far field data. For numerical applications arbitrarily shaped smooth cylinders from the following table are used.

Contour Type:	Parametric Representation:
Apple Shaped	$\Gamma^{(a)} = \left\{ \frac{0.5 + 0.4\cos \boldsymbol{t} + 0.1\sin 2\boldsymbol{t}}{1 + 0.7\cos \boldsymbol{t}} (\cos \boldsymbol{t}, \sin \boldsymbol{t}) : \boldsymbol{t} \in [0, 2\pi] \right\}$
Circle	$\Gamma^{(c)} = \{ \boldsymbol{c}_0 (\cos \boldsymbol{t}, \sin \boldsymbol{t}) : \boldsymbol{t} \in [0, 2\pi] \}$, $\boldsymbol{c}_0$: constant
Ellipse	$\Gamma^{(e)} = \{ (\boldsymbol{e}_0 \cos \boldsymbol{t}, \boldsymbol{e}_1 \sin \boldsymbol{t}) : \boldsymbol{t} \in [0, 2\pi] \}$, $\boldsymbol{e}_0, \boldsymbol{e}_1$: constant
Peanut Shaped	$\Gamma^{(p)} = \left\{ \sqrt{\cos^2 \boldsymbol{t} + 0.25\sin^2 \boldsymbol{t}} (\cos \boldsymbol{t}, \sin \boldsymbol{t}) : \boldsymbol{t} \in [0, 2\pi] \right\}$
Rounded Rectangle	$\Gamma^{(r)} = \left\{ 0.6 \left(\sin^{10} \boldsymbol{t} + \left(\frac{2}{3} \cos \boldsymbol{t} \right)^{10} \right)^{-0.1} (\cos \boldsymbol{t}, \sin \boldsymbol{t}) : \boldsymbol{t} \in [0, 2\pi] \right\}$
Rounded Triangle	$\Gamma^{(t)} = \{ (0.5 + 0.075\cos \boldsymbol{t})(\cos \boldsymbol{t}, \sin \boldsymbol{t}) : \boldsymbol{t} \in [0, 2\pi] \}$

Table1: Parametric Representation of Boundary Curves

In the first example, an apple shaped sound soft obstacle is buried in a circular penetrable cylinder with a radius $\boldsymbol{c}_0 = 0.8$. Wave numbers for corresponding mediums are $\boldsymbol{k}_0 = 1.5$, $\boldsymbol{k}_1 = 0.5$ and the scatterers are illuminated from the direction $\phi_0 = 180^0$. $\Gamma^{(0)}$ is chosen as a circle with $\boldsymbol{c}_0 = 0.2$. The conductivity function over the boundary Γ_1 is taken as $\lambda(\boldsymbol{t}) = 1 + \sin^3 \boldsymbol{t} + \boldsymbol{i}\sin \boldsymbol{t}$ for $\boldsymbol{t} \in [0, 2\pi]$. For the exact data Tikhonov regularization parameters $\alpha_1 = 10^{-14}$, $\alpha_2 = 7\times10^{-3}$ and for the noisy case $\alpha_1 = 8\times10^{-2}$, $\alpha_2 = 9\times10^{-2}$ are chosen. The degree of the polynomials $\boldsymbol{R} = 4$ and $\boldsymbol{R} = 2$ are used for exact and noisy data, respectively.

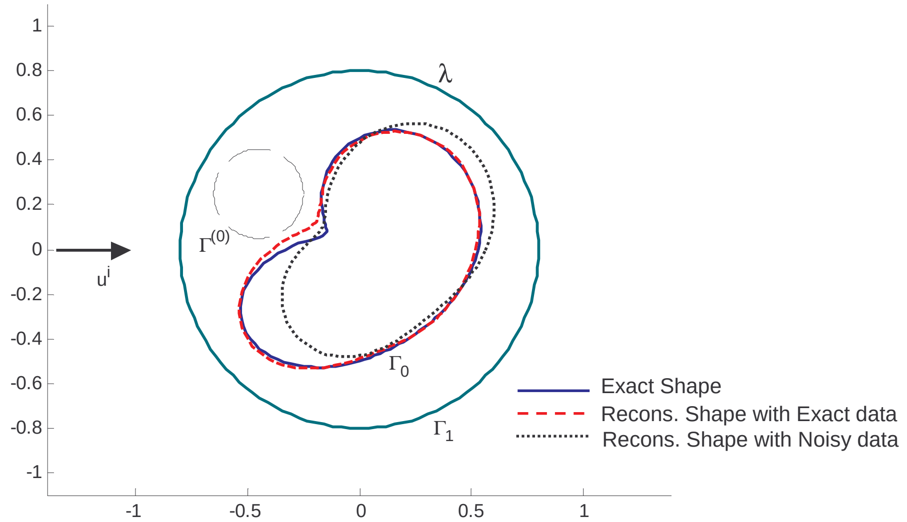

Figure1: Reconstruction of an apple shaped obstacle buried in a circular cylinder

As a second example buried obstacle is considered a rounded triangular shaped scatterer and the cylinder is a rounded rectangular shaped object. The incident angle is $\phi_0 = 0^0$, and the wave numbers are $\boldsymbol{k}_0 = 3$, $\boldsymbol{k}_1 = 2$. We choose initially guessed boundary as a circle with radius $\boldsymbol{c}_0 = 0.2$ in the shadow region and choose $\lambda = 0$ to investigate the affects of these two parameters to the reconstructions. Therefore, boundary conditions in (2) are reduced to transmission conditions. The regularization parameters are chosen as $\alpha_1 = 10^{-14}$, $\alpha_2 = 10^{-2}$, $\boldsymbol{R} = 4$ for exact data and $\alpha_1 = 10^{-4}$, $\alpha_2 = 8\times10^{-2}$, $\boldsymbol{R} = 3$ for noisy case.

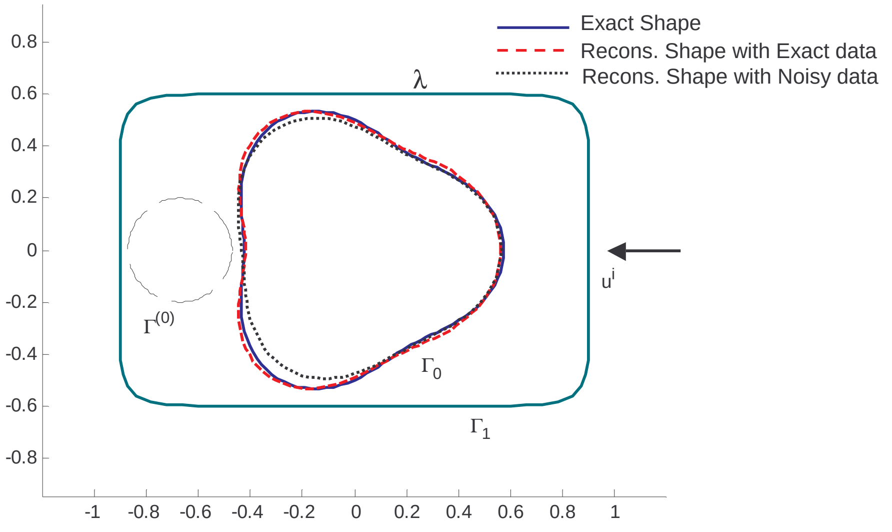

Figure2: Reconstruction of a rounded triangular shaped obstacle buried in a rounded rectangle

In the final example we tried to test the reconstruction method with limited far field data. To this aim a peanut shaped obstacle is buried in an elliptic cylinder having constant parameters $\boldsymbol{e}_0 = 1.8$, $\boldsymbol{e}_1 = 1.2$ where the configuration is illuminated from the direction $\phi_0 = 0^0$. Then the far field data collected on a semi circle $\Omega^{\boldsymbol{m}}$ for $\phi \in [0,\pi]$. Wave numbers for corresponding background mediums are $\boldsymbol{k}_0 = 2$, $\boldsymbol{k}_1 = 1$. The conductivity function is chosen $\lambda(\boldsymbol{t}) = \sin^4 \boldsymbol{t}/2 + \boldsymbol{i}\cos^4 \boldsymbol{t}/2$ for $\boldsymbol{t} \in [0,2\pi]$ on Γ_1. Here, $\Gamma^{(0)} = \Gamma^{(\boldsymbol{c})}$ is chosen with radius $\boldsymbol{c}_0 = 0.4$ in the symmetry center of the scatterers. Regularization parameters are set as $\alpha_1 = 10^{-14}$, $\alpha_2 = 10^{-3}$, $\boldsymbol{R} = 4$ and $\alpha_1 = 10^{-5}$, $\alpha_2 = 2\times10^{-2}$, $\boldsymbol{R} = 2$ for the exact data and noisy data cases, respectively.

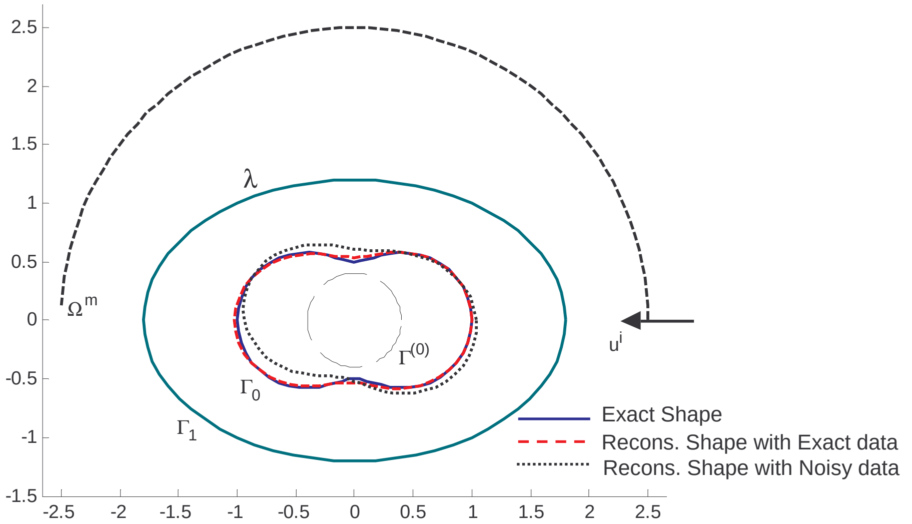

Figure3: Reconstruction of a peanut shaped obstacle buried in an elliptic cylinder

6 CONCLUSIONS

The applicability and the effectiveness of the method is supported by the numerical results. As to be expected, exact data with good initial guess gives better reconstructions with various wave numbers in the resonance region. In the case of noise level exceeds $(3\% - 4\%)$ the results start to deteriorate. Moreover, for the exact data case we generally need small Tikhonov regularization parameters and higher degree of polynomials, but for the noisy data we need stronger regularization parameters and lower degree of polynomials[3,4]. It can also be concluded that when the conductivity function over the penetrable cylinder vanishes, one can get the best reconstructions with full exact far field data even the initial guess is located in the shadow region. The illumination angle and the iteration numbers play an important role for the quality of the reconstructions due to the geometry of the configuration. It is also observed that higher iteration numbers is needed to reconstruct more complex objects.

Finally, we expect that the proposed method can be extended to multi-layered case and for two-dimensional cracks.

7 REFERENCES

1. D. Colton and R. Kress: Inverse Acoustic and Electromagnetic Scattering Theory, 2nd ed Springer, Berlin (1998).
2. R.Kress,'Newton's Method for inverse obstacle scattering meets the method of least squares.' Inverse Problems, 19, 91-104 (2003).
3. R Kress, F. Yaman, A. Yapar and I. Akduman, 'Inverse scattering for an impedance cylinder buried in a dielectric cylinder' submitted to Inverse Problems in Science and Engineering (2007).
4. F.Yaman, 'Location and Shape Reconstruction Problems for Sound-Soft Obstacles Buried in Cylinders' submitted to IEEE Transactions on Geoscience and Remote Sensing (2008)

Acknowledgment: The main part of this research was carried out while Fatih Yaman was visiting the University of Göttingen as a fellow of Deutsche Akademische Auslandsdienst (DAAD). The hospitality of the University of Göttingen and the support of the DAAD are gratefully acknowledged.